SUPPORTING INFORMATION

Antisite Disorder and Bond Valence Compensation in Li_2FePO_4F Cathode for Li-ion Batteries.

Olesia M. Karakulina[†], Nellie R. Khasanova[‡], Oleg A. Drozhzhin[‡,§], Alexander A. Tsirlin[||,⊥], Joke Hadermann[†], Evgeny V. Antipov[‡] and Artem M. Abakumov[§,†]

[†]EMAT, University of Antwerp, Groenenborgerlaan 171, B-2020, Antwerp, Belgium

[‡]Department of Chemistry, Lomonosov Moscow State University, 119991 Moscow, Russia

[§]Skoltech Center for Electrochemical Energy Storage, Skolkovo Institute of Science and Technology, Nobel str. 3, 143026 Moscow, Russia

[||]Experimental Physics VI, Center for Electronic Correlations and Magnetism, University of Augsburg, 86159 Augsburg, Germany

[⊥]National Institute of Chemical Physics and Biophysics, Akadeemia tee 23, 12618 Tallinn, Estonia

MATERIAL SYNTHESIS AND CHARACTERIZATION

The $LiNaFePO_4F$ samples for electrochemical exchange were prepared by two-step synthesis. First, $LiFePO_4$ was obtained by solid state reaction and then it was annealed with NaF in 1:1 ratio at 670°C for 1 hour under Ar-flow. A planetary ball milling machine (Fritsch Pulverisette 7 with WC bowl) was used for the initial mixing of reagents and for intermediate regrindings. $Li_{1.13}Na_{0.87}FePO_4F$ and $Li_{1.68}Na_{0.32}FePO_4F$ were prepared from $LiNaFePO_4F$ by chemical exchange with 1.5× excess of LiBr in dry acetonitrile at room temperature. The obtained products were washed in acetonitrile and dried in air.

For electrochemical cation exchange positive electrodes were produced by thorough mixing of 75 wt% active material ($LiNaFePO_4F$), 15 wt% carbon black (Carbon Super-C) and 10 wt% polyvinylidene fluoride (PVdF) binder dissolved in N-methyl-pyrrolidone. The slurry was uniformly cast on the Al foil by Doctor Blade technique with a loading of 1-3 mg/cm^2 and roll-pressed. Round-shaped electrodes (ø10 mm) were cut out, weighed and dried at 80°C under low pressure (10^{-2} mbar.) for 4 hours to remove the residual water and solvent.

Electrochemical cation exchange was performed with a Biologic VMP-3 (EC-Lab) potentiostat-galvanostat in two-electrode clamping cells assembled in an Ar-filled glovebox (MBraun, Germany) with Li-foil as a counter electrode (anode) and a solution of 1M $LiBF_4$ in tetramethylene sulfone (TMS) served as electrolyte. Borosilicate glass fiber was used as a separator. The cation exchange was carried out by cycling of the $LiNaFePO_4F$ cathodes 10 times within the potential range of 2.6–4.0 V *vs* Li/Li^+ followed by a discharge to 2.6V. The exchange was performed at 75°C and at room temperature for Li_2FePO_4F-75 and Li_2FePO_4F-RT, respectively. Li_2FePO_4F-75 demonstrates initial discharge capacity of ~112 mAh/g with a capacity fade to ~95 mAh/g after 10 charge/discharge cycles. (Figure S1, a).

The $LiFePO_4$ samples for the electrochemical study were prepared with a simple hydrothermal route using LiOH, $FeSO_4$ and H_3PO_4 solutions in molar ratio 3:1:1 heated at 190^{o}C for 3 h. Electrochemical cycling at 100 ^{o}C was performed using the same experimental setup as for the Li_2FePO_4F samples; the applied potential range was 2.2-4.1 V *vs*. Li/Li^+ (Figure S1, b). $LiFePO_4$ exhibits the initial discharge capacity of ~150 mAh/g without a noticeable fade during the cycling.

The samples were characterized by powder X-ray diffraction (PXRD) using a Huber G670 Guinier camera ($CuK_{\alpha 1}$-radiation, Ge monochromator, image plate detector) and a Bruker D2 PHASER with a Lynxeye detector (CoK_α-radiation). High-resolution synchrotron X-ray powder diffraction (SXPD) data for the chemically substituted $Li_xNa_{2-x}FePO_4F$ samples were collected at room temperature at the ID31 beamline of the European Synchrotron Radiation Facility (ESRF, Grenoble, France) using a constant

wavelength of λ ≈ 0.4 Å and eight scintillation detectors, each preceded by a Si(111) analyzer crystal. The powder samples were placed in a borosilicate glass capillary that was spun during the experiment. The Rietveld refinement of the $Li_xNa_{2-x}FePO_4F$ structures was performed in the JANA2006 program package [1]. The crystallographic data are presented in Table S8, the atomic parameters and main interatomic distances are listed in Tables S9-S14. The experimental, calculated and difference SXPD patterns are shown in Figure 6.

The TEM study was performed with FEI Tecnai G2 and FEI Osiris electron microscopes operated at 200 kV and equipped with a Super-X detector. The specimens were prepared in air-free condition by dispersing the materials in dry hexane and depositing a drop of suspension on a holey carbon grid. A Gatan double-tilt vacuum transfer holder was used to transfer the samples to the microscope column without contact with air. The parameters of the electron diffraction tomography experiments are listed in Table S1. The data were treated with the PETS software [2].

By means of selected area electron diffraction (SAED, Figure S2, a) of Li_2FePO_4F-75 the reflection conditions *hk0: h*=2n, *0kl: k+l*=2n were determined corroborating the *Pnma* (№62) space group. The $LiNaFePO_4F$ structure [3] with Na at the 8*d* position replaced by Li was used as the initial model. No Na was observed in this sample by EDX analysis (Figure S3). The refinement with the common atomic displacement parameter (ADP) for all atoms revealed the reliability factor R_F = 0.295. The refinement of the ADPs for the Li and Fe positions separately demonstrated negative ADP for the position Li2 (U_{iso} = -0.014(2)Å^2) and large positive ADPs for the Fe positions (U_{iso} = 0.032(1)Å^2). This can indicate underestimated scattering density at the Li2 position and overestimated scattering density at the Fe position pointing to the Li/Fe antisite disorder. An additional confirmation is found on difference Fourier maps showing positive peaks at the Li positions and negative peaks at the Fe positions (Fig. 1 of the Article). The refinement of the Li/Fe occupancy factors for the 3 Li and 2 Fe positions reduced the reliability factor down to R_F = 0.219, brought ADPs back to normal, and resulted in the $Li_{1.96(6)}Fe_{1.04(6)}PO_4F$ composition, in good agreement with the nominal composition of the material. A noticeably better agreement with the experimental data can be also seen from F_{obs}-F_{calc} plot for the ordered and disordered models (Figure S5). Final refinement was performed with the occupancy factors restrained to the nominal Li_2FePO_4F composition and common ADP for the Li and Fe positions.

Apart from Li_2FePO_4F-75, the SAED diffraction pattern along the [100] direction of Li_2FePO_4F-RT has weak reflections contradicting *n*-glide plane (0*kl*, *k+l*≠2n) (Figure S2, b). Therefore, the structure refinement in the $P2_1ma$ space group (acentric subgroup of *Pnma*) was attempted. However, it did not result in any change in the occupancy factors and did not improve the reliability factor compared to the *Pnma* model, despite the fact that the number of refineable parameters increased. The absence of the *n*-plane may be caused by minor atomic displacements, which are too small to be detected in EDT. Therefore, the Li_2FePO_4F-RT structure was refined in the *Pnma* group. Additionally, Na was added to the Li1 position, as a small fraction of Na was detected in this sample by EDX analysis. The EDX analysis was performed in TEM on 19 different crystallites using the Na-K line and the measured Na content corresponds to the $Li_{1.84}Na_{0.16(3)}FePO_4F$ formula (Figure S4).

Contrary to the Li_2FePO_4F structures, the refinement of $LiFePO_4$-100 revealed a complete absence of the antisite disorder. Crystallographic information on the Li_2FePO_4F-75, Li_2FePO_4F-RT, and $LiFePO_4$-100 structures is summarized in Table S1, the atomic parameters are presented in the Tables S2, S4, S6, and main interatomic distances – in Tables S3, S5, and S7, respectively.

DEFECT ENERGY CALCULATION

Energies of antisite defects were obtained from density-functional (DFT) band-structure calculations performed in the VASP code [4,5]. The Perdew-Burke-Ernzerhof version of the exchange-correlation potential was used [6]. Correlations effects in the Fe 3d shell were taken into account on the DFT+*U* level with the on-site Coulomb repulsion *U* = 5 eV and Hund's exchange *J* = 1 eV [7]. All calculations for Li_2FePO_4F and delithiated $LiFePO_4F$ were performed on a 2x2x2 k-mesh with 8 k-points in the first Brillouin zone. Convergence with respect to the k-points was checked by increasing the number of k-points to 27 (3x3x3 mesh), and no significant changes in defect energies were found. To exclude the

effect of magnetism on the calculated energies, ferromagnetic spin configuration was assumed in all calculations.

Experimental lattice parameters *a* = 10.581 Å, *b* = 6.211 Å, *c* = 10.937 Å were used. Defect configurations were generated by swapping positions of individual Li and Fe atoms. 16 different configurations that are possible within the 64-atom crystallographic unit cell of delithiated $LiFePO_4F$ were considered. For each configuration, all atomic positions were relaxed until residual forces were below 0.01 eV/Å. Defect formation energy was calculated as the difference between the energy of a given defect structure and the energy of the parent structure without defects. Such energies include the energy cost of accommodating Fe in the Li position and Li in the position of Fe. If, on the other hand, only the migration of Fe into the Li position is considered, the results will not reflect changes in lattice energy upon subsequent Li intercalation. Our calculations suggest the proclivity of $LiFePO_4F$ to the formation of antisite defects, i.e., to the simultaneous filling of Li positions with Fe and Fe positions with Li, thus explaining capacity fade observed experimentally.

For comparison, we calculated defect energies for $LiFePO_4$, where Fe and Li positions are unique. This gives rise to 4 possible defect configurations producing two pairs of equivalent structures. Their energies of 0.65 eV and 0.72 eV, respectively, are generally consistent with the values of 0.74 eV [8] and 0.55 eV [7] reported in the previous literature.

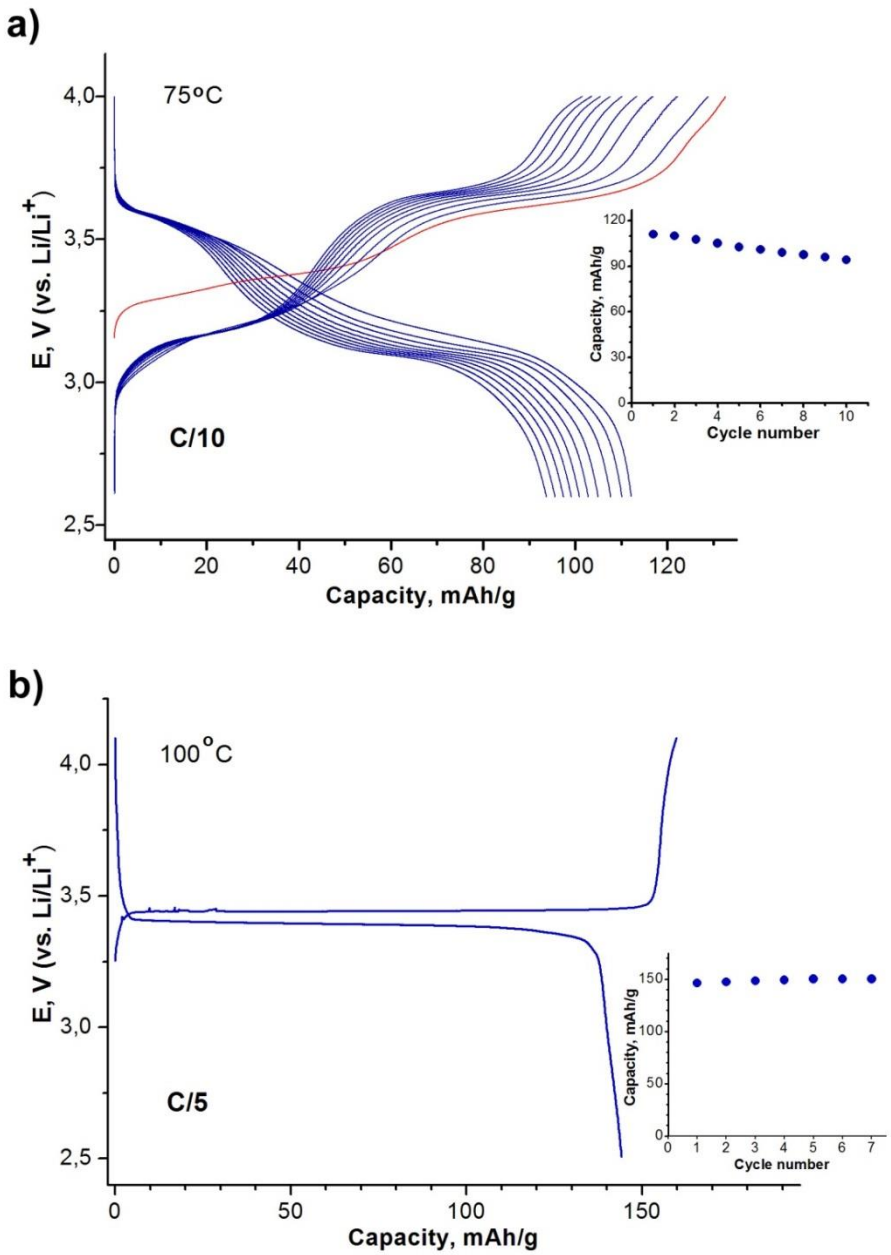

Figure S1. Charge-discharge curves and capacity retention of Li_2FePO_4F (a) and $LiFePO_4$ (b) samples at 75 ^oC and 100 ^oC, respectively. Red curve corresponds to the charging of the initial $LiNaFePO_4F$ phase, which transforms to Li_2FePO_4F upon subsequent cycling.

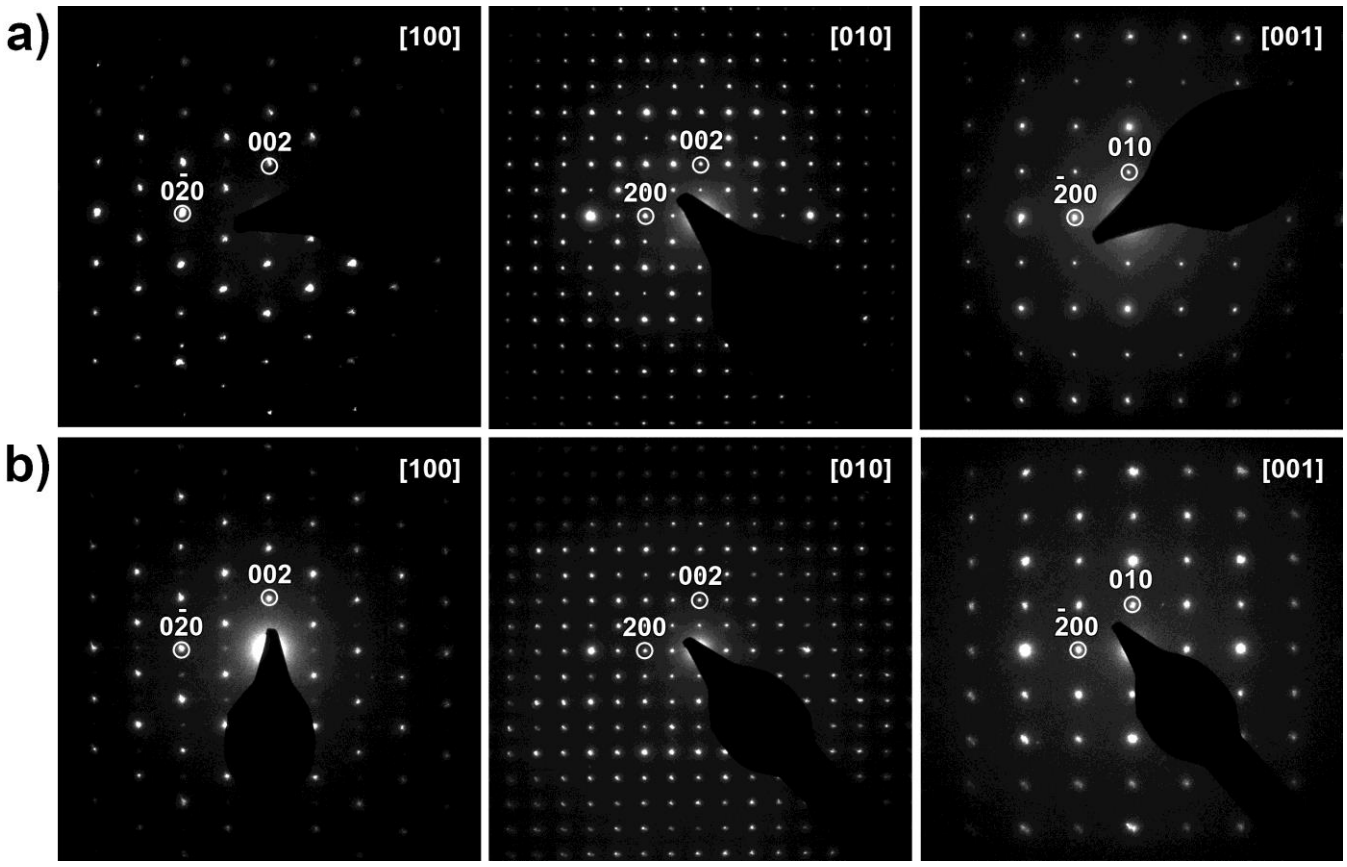

Figure S2.Selected area electron diffraction patterns of Li_2FePO_4F-75 (a) and Li_2FePO_4F-RT (b).

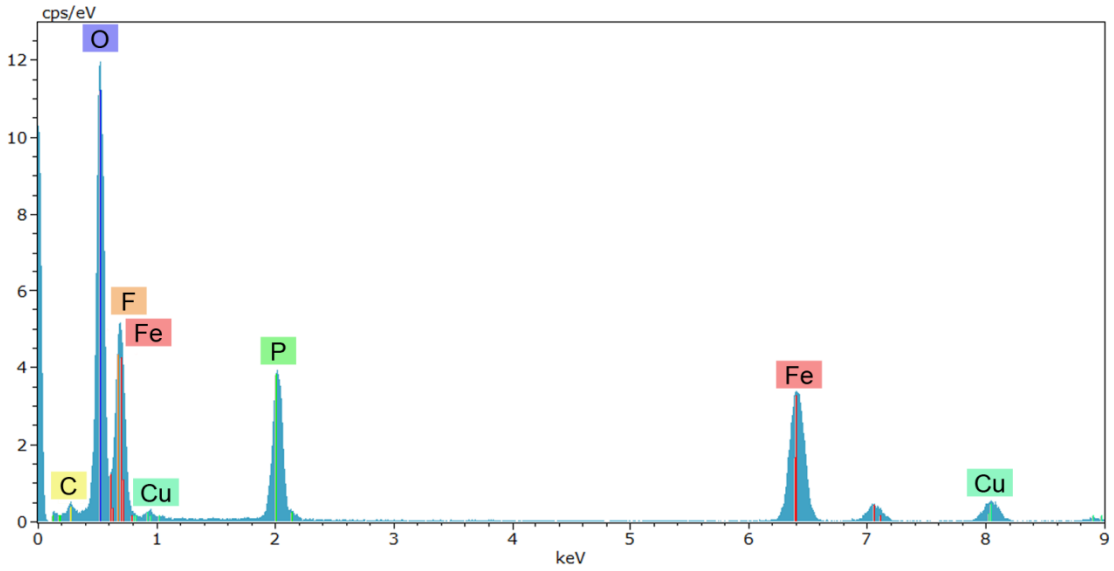

Figure S3. Typical EDX spectrum of the Li_2FePO_4F-75 sample demonstrating the absence of sodium. The Cu signal originates from the sample support.

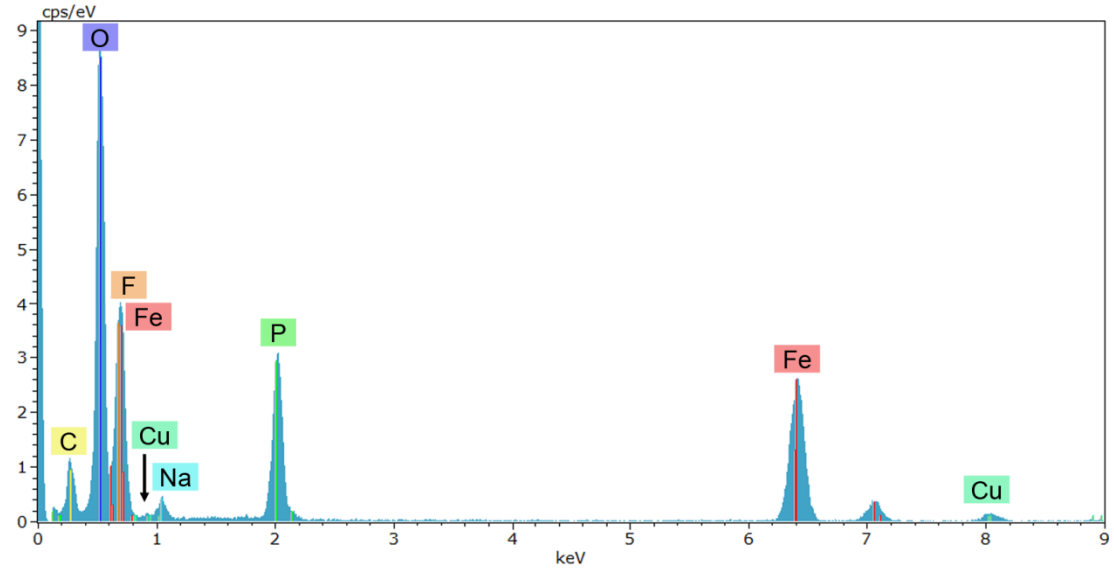

Figure S4. EDX spectrum of the Li_2FePO_4F-RT sample demonstrating small residual Na-K peak. The Cu signal originates from the sample support.

Table S1**.** Crystallographic data and refinement parameters for the Li_2FePO_4F-75, Li_2FePO_4F-RT, and $LiFePO_4$-100 structures by means of electron diffraction tomography.

Sample	Li_2FePO_4F-75	Li_2FePO_4F-RT	$LiFePO_4$-100
Formula	Li_2FePO_4F	$Li_{1.84}Na_{0.16}FePO_4F$	$LiFePO_4$
Space group	*Pnma*	*Pnma*	*Pnma*
a, Å	10.4171(5)[1]	10.4465(4)[2]	10.3100(4)[1]
b, Å	6.4796(7)[1]	6.4815(4)[2]	6.0092(3)[1]
c, Å	10.954(2)[1]	10.9805(7)[2]	4.6848(2)[1]
V, Å^3	739.4(1)	743.5(1)	290.24(1)
Z	8	8	4
ρ, g/cm^3	3.284	3.328	3.602
Radiation	Electron	Electron	Electron
	λ = 0.0251 Å	λ = 0.0251 Å	λ = 0.0251 Å
Scanned angular range, deg.	110	125	124
Number of independent reflections (I > 3s(I))	1088	935	369
Parameters refined	37	37	17
R_F	0.219	0.283	0.188

[1] - unit cell parameters determined from PXRD data with the LeBail fit;
[2] - unit cell parameters from Ref. 1;

Table S2. Fractional atomic coordinates, atomic displacement parameters for Li_2FePO_4F-75.

Atom	Position	Occupancy	*x/a*	*y/b*	*z/c*	U_{iso}, Å^2
Li1	8*d*	0.903(7)Li 0.097(7)Fe	0.7538(9)	0.968(2)	0.6510(9)	0.0174(7)
Li2	4*c*	0.63(1)Li 0.37(1)Fe	0.9734(7)	3/4	0.7154(7)	0.0174(7)
Li3	4*c*	0.91(1)Li 0.09(1)Fe	0.284(1)	1/4	0.582(1)	0.0174(7)
Fe1	4*a*	0.73(2)Fe 0.27(2)Li	0	0	0	0.0174(7)
Fe2	4*b*	0.62(1)Fe 0.38(1)Li	0	0	1/2	0.0174(7)
P1	4*c*	1	0.7563(5)	3/4	0.9191(4)	0.0119(8)
P2	4*c*	1	0.0228(4)	1/4	0.7445(5)	0.0119(8)
O1	8*d*	1	0.8113(6)	0.942(1)	0.9811(5)	0.0189(7)
O2	4*c*	1	0.6119(8)	3/4	0.9402(8)	0.0189(7)
O3	4*c*	1	0.7873(8)	3/4	0.7838(8)	0.0189(7)
O4	8*d*	1	-0.0297(6)	0.443(1)	0.6792(5)	0.0189(7)
O5	4*c*	1	0.1693(8)	1/4	0.7413(8)	0.0189(7)
O6	4*c*	1	-0.0258(8)	1/4	0.8768(8)	0.0189(7)
F1	4*c*	1	0.0603(8)	3/4	0.8788(7)	0.0189(7)
F2	4*c*	1	0.8699(8)	3/4	0.5361(8)	0.0189(7)

Table S3. Selected interatomic distances (Å) for Li_2FePO_4F-75.

Bond		Bond	
Li1-O1	2.065(12)	Fe1-O1	2.012(6) ×2
Li1-O3	2.059(13)	Fe1-O6	2.125(6) ×2
Li1-O4	2.348(12)	Fe1-F1	2.187(5) ×2
Li1-O5	2.344(13)		
Li1-F1	2.485(12)	Fe2-O2	2.100(5) ×2
Li1-F2	2.247(13)	Fe2-O4	2.022(6) ×2
		Fe2-F2	2.149(5) ×2
Li2-O2	2.233(11)		
Li2-O3	2.078(11)		
Li2-O4	2.031(8) ×2	P1-O1	1.527(8) ×2
Li2-F1	2.005(11)	P1-O2	1.523(10)
Li2-F2	2.241(11)	P1-O3	1.517(10)
Li3-O1	2.133(9) ×2	P2-O4	1.539(8) ×2
Li3-O5	2.11(2)	P2-O5	1.526(10)
Li3-O6	2.04(2)	P2-O6	1.536(10)
Li3-F1	2.76(2)		
Li3-F2	2.05(2)		

Table S4. Fractional atomic coordinates, atomic displacement parameters for Li_2FePO_4F-RT.

Atom	Position	Occupancy	*x/a*	*y/b*	*z/c*	U_{iso}, Å^2
Li1	8*d*	0.63(1)Li 0.21(1)Fe 0.16Na	0.752(1)	0.979(3)	0.659(1)	0.020(1)
Li2	4*c*	0.73(2)Li 0.27(2)Fe	0.977(2)	3/4	0.720(2)	0.020(1)
Li3	4*c*	0.94(2)Li 0.06(2)Fe	0.258(3)	1/4	0.573(3)	0.020(1)
Fe1	4*a*	0.65(5)Fe 0.35(5)Li	0	0	0	0.020(1)
Fe2	4*b*	0.59(2)Fe 0.41(2)Li	0	0	½	0.020(1)
P1	4*c*	1	0.7572(7)	3/4	0.9227(7)	0.003(1)
P2	4*c*	1	0.0220(7)	1/4	0.7431(7)	0.003(1)
O1	8*d*	1	0.8120(9)	0.942(1)	0.9828(9)	0.0135(9)
O2	4*c*	1	0.614(1)	3/4	0.945(1)	0.0135(9)
O3	4*c*	1	0.787(1)	3/4	0.787(1)	0.0135(9)
O4	8*d*	1	-0.0427(9)	0.442(2)	0.6805(9)	0.0135(9)
O5	4*c*	1	0.164(1)	1/4	0.742(1)	0.0135(9)
O6	4*c*	1	-0.031(1)	1/4	0.876(1)	0.0135(9)
F1	4*c*	1	0.067(1)	3/4	0.880(1)	0.0135(9)
F2	4*c*	1	0.864(1)	3/4	0.539(1)	0.013(1)

Table S5. Selected interatomic distances (Å) for Li_2FePO_4F-RT.

Bond		Bond	
Li1-O1	2.10(2)	Fe1-O1	2.001(10) ×2
Li1-O3	2.08(2)	Fe1-O6	2.140(9) ×2
Li1-O4	2.22(2)	Fe1-F1	2.203(9) ×2
Li1-O5	2.26(2)		
Li1-F1	2.48(2)	Fe2-O2	2.098(8) ×2
Li1-F2	2.31(2)	Fe2-O4	2.066(10) ×2
		Fe2-F2	2.196(9) ×2
Li2-O2	2.30(2)		
Li2-O3	2.12(2)	P1-O1	1.557(13) ×2
Li2-O4	2.053(14) ×2	P1-O2	1.52(2)
Li2-F1	1.99(2)	P1-O3	1.52(2)
Li2-F2	2.31(2)		
		P2-O4	1.574(13) ×2
Li3-O1	2.12(2) ×2	P2-O5	1.49(2)
Li3-O5	2.10(3)	P2-O6	1.56(2)
Li3-O6	2.28(3)		
Li3-F1	2.79(3)		
Li3-F2	1.77(3)		

Table S6. Fractional atomic coordinates, atomic displacement parameters for $LiFePO_4$-100.

Atom	Position	Occupancy	*x/a*	*y/b*	*z/c*	U_{iso}, Å^2
Li1	*4b*	1.00(2)Li	1/2	1/2	0	0.014(2)
Fe1	4*c*	1.00(2)Fe	0.2166(5)	3/4	0.024(1)	0.014(2)
P1	4*c*	1	0.4057(7)	3/4	0.582(2)	0.007(2)
O1	8*d*	1	0.3354(8)	0.952(2)	0.717(2)	0.015(2)
O2	4*c*	1	0.5453(9)	3/4	0.707(3)	0.015(2)
O3	4*c*	1	0.409(1)	3/4	0.252(2)	0.015(2)

Table S7. Selected interatomic distances (Å) for $LiFePO_4$-100.

Bond		Bond	
Li1-O1	2.174(9) ×2	Fe1-O1	2.077(9) ×2
Li1-O2	2.086(10) ×2	Fe1-O1	2.246(10) ×2
Li1-O3	2.131(8) ×2	Fe1-O2	2.074(12)
		Fe1-O3	2.249(13)
		P1-O1	1.547(10) ×2
		P1-O2	1.555(13)
		P1-O3	1.543(12)

Table S8**.** Crystallographic data and refinement parameters for the $Li_xNa_{2-x}FePO_4F$ structures refined from synchrotron X-ray powder diffraction data.

Formula	$Li_{0.97}Na_{1.03}FePO_4F$	$Li_{1.13}Na_{0.87}FePO_4F$	$Li_{1.68}Na_{0.32}FePO_4F$
Space group	*Pnma*	*Pnma*	*Pnma*
a, Å	10.98346(3)	10.64163(3)	10.5199(1)
b, Å	6.36002(3)	6.52292(2)	6.50471(7)
c, Å	11.43011(3)	11.28387(5)	11.0597(2)
V, $Å^3$	798.450(3)	783.265(3)	756.81(1)
Z	8	8	8
ρ, g/cm^3	3.329	3.351	3.313
Radiation	Synchrotron X-ray	Synchrotron X-ray	Synchrotron X-ray
	λ = 0.39996 Å	λ = 0.39996 Å	λ = 0.39996 Å
2θ range, deg.	2 - 30	2.3 – 30.6	2.3 – 20.8
Number of reflections	985	1021	323
Parameters refined	35	35	34
R_F, R_P, R_{wP}	0.024, 0.075, 0.098	0.032, 0.072, 0.095	0.022, 0.066, 0.085

Table S9. Fractional atomic coordinates, atomic displacement parameters for $Li_{0.97}Na_{1.03}FePO_4F$.

Atom	Position	Occupancy	*x/a*	*y/b*	*z/c*	U_{iso}, $Å^2$
Na1	8*d*	0.997(6)Na 0.003(6)Li	0.7742(2)	0.9911(5)	0.6532(2)	0.0161(9)
Li2	4*c*	0.941(6)Li 0.059(6)Na	0.039(1)	3/4	0.730(1)	0.0161(9)
Li3	4*c*	1	0.277(2)	1/4	0.594(2)	0.0161(9)
Fe1	4*a*	1	0	0	0	0.0074(2)
Fe2	4*b*	1	0	0	1/2	0.0074(2)
P1	4*c*	1	0.7549(3)	3/4	0.9201(2)	0.0051(4)
P2	4*c*	1	0.0414(2)	1/4	0.7426(3)	0.0051(4)
O1	8*d*	1	0.8196(3)	0.9519(5)	0.9635(3)	0.0078(4)
O2	4*c*	1	0.6262(4)	3/4	0.9831(5)	0.0078(4)
O3	4*c*	1	0.7387(5)	3/4	0.7878(4)	0.0078(4)
O4	8*d*	1	-0.0089(4)	0.4509(6)	0.6810(2)	0.0078(4)
O5	4*c*	1	0.1807(4)	1/4	0.7393(6)	0.0078(4)
O6	4*c*	1	-0.0106(5)	1/4	0.8698(5)	0.0078(4)
F1	4*c*	1	0.0623(4)	3/4	0.8936(4)	0.0078(4)
F2	4*c*	1	0.8696(4)	3/4	0.5257(4)	0.0078(4)

Table S10. Selected interatomic distances (Å) for $Li_{0.97}Na_{1.03}FePO_4F$.

Bond		Bond	
Na1-O1	2.428(4)	Fe1-O1	2.047(3) ×2
Na1-O2	2.773(5)	Fe1-O6	2.181(4) ×2
Na1-O3	2.207(4)	Fe1-F1	2.116(3) ×2
Na1-O4	2.432(4)		
Na1-O5	2.297(5)	Fe2-O2	2.119(3) ×2
Na1-F1	2.838(5)	Fe2-O4	2.095(3) ×2
Na1-F2	2.361(4)	Fe2-F2	2.160(3) ×2
Li2-O2	2.617(16)	P1-O1	1.549(4) ×2
Li2-O3	2.204(14)	P1-O2	1.586(6)
Li2-O4	2.051(6) ×2	P1-O3	1.523(5)
Li2-F1	1.888(16)		
Li2-F2	2.984(15)	P2-O4	1.560(4) ×2
		P2-O5	1.530(5)
Li3-O1	2.060(7) ×2	P2-O6	1.563(6)
Li3-O5	1.970(18)		
Li3-O6	2.369(18)		
Li3-F1	2.891(17)		
Li3-F2	2.113(17)		

Table S11. Fractional atomic coordinates, atomic displacement parameters for $Li_{1.13}Na_{0.87}FePO_4F$.

Atom	Position	Occupancy	*x/a*	*y/b*	*z/c*	U_{iso}, Å^2
Na1	8*d*	0.806(5)Na 0.194(5)Li	0.7499(3)	0.9886(6)	0.6588(3)	0.0240(9)
Li2	4*c*	0.873(6)Li 0.127(6)Na	0.9627(6)	3/4	0.738(1)	0.0240(9)
Li3	4*c*	1	0.266(2)	1/4	0.585(2)	0.0240(9)
Fe1	4*a*	1	0	0	0	0.0085(2)
Fe2	4*b*	1	0	0	1/2	0.0085(2)
P1	4*c*	1	0.7584(2)	3/4	0.9180(3)	0.0064(4)
P2	4*c*	1	0.0207(2)	1/4	0.7404(3)	0.0064(4)
O1	8*d*	1	0.8143(3)	0.9453(5)	0.9774(4)	0.0104(4)
O2	4*c*	1	0.6148(5)	3/4	0.9442(4)	0.0104(4)
O3	4*c*	1	0.7884(4)	3/4	0.7875(4)	0.0104(4)
O4	8*d*	1	-0.0324(3)	0.4483(5)	0.6785(3)	0.0104(4)
O5	4*c*	1	0.1647(5)	1/4	0.7363(6)	0.0104(4)
O6	4*c*	1	-0.0199(5)	1/4	0.8723(5)	0.0104(4)
F1	4*c*	1	0.0664(4)	3/4	0.8831(4)	0.0104(4)
F2	4*c*	1	0.8662(4)	3/4	0.5267(4)	0.0104(4)

Table S12. Selected interatomic distances (Å) for $Li_{1.13}Na_{0.87}FePO_4F$.

Bond		Bond	
Na1-O1	2.201(5)	Fe1-O1	2.024(3) ×2
Na1-O3	2.168(5)	Fe1-O6	2.186(4) ×2
Na1-O4	2.364(5)	Fe1-F1	2.213(3) ×2
Na1-O5	2.265(5)		
Na1-F1	2.541(5)	Fe2-O2	2.133(3) ×2
Na1-F2	2.485(5)	Fe2-O4	2.071(4) ×2
		Fe2-F2	2.186(3) ×2
Li2-O2	2.615(12)		
Li2-O3	1.938(8)	P1-O1	1.557(4) ×2
Li2-O4	2.079(6) ×2	P1-O2	1.557(6)
Li2-F1	1.977(13)	P1-O3	1.507(6)
Li2-F2	2.593(14)		
Li3-O1	2.172(9) ×2	P2-O4	1.575(4) ×2
Li3-O5	2.02(2)	P2-O5	1.533(6)
Li3-O6	2.329(17)	P2-O6	1.549(6)
Li3-F1	2.90(2)		
Li3-F2	1.89(2)		

Table S13. Fractional atomic coordinates, atomic displacement parameters for $Li_{1.68}Na_{0.32}FePO_4F$.

Atom	Position	Occupancy	*x/a*	*y/b*	*z/c*	U_{iso}, Å^2
Na1	8*d*	0.319(6)Na 0.681(6)Li	0.750(1)	0.992(1)	0.6657(5)	0.016(2)
Li2	4*c*	1	0.960(2)	3/4	0.750(4)	0.016(2)
Li3	4*c*	1	0.251(3)	1/4	0.581(3)	0.016(2)
Fe1	4*a*	1	0	0	0	0.0067(3)
Fe2	4*b*	1	0	0	1/2	0.0067(3)
P1	4*c*	1	0.7574(5)	3/4	0.9157(4)	0.0064(4)
P2	4*c*	1	0.0193(5)	1/4	0.7410(5)	0.0064(4)
O1	8*d*	1	0.8100(4)	0.9386(6)	0.9764(4)	0.0061(4)
O2	4*c*	1	0.6160(5)	3/4	0.9306(7)	0.0061(4)
O3	4*c*	1	0.7933(8)	3/4	0.7861(6)	0.0061(4)
O4	8*d*	1	-0.0342(5)	0.4421(7)	0.6798(4)	0.0061(4)
O5	4*c*	1	0.1705(8)	1/4	0.7356(8)	0.0061(4)
O6	4*c*	1	-0.0225(8)	1/4	0.8735(9)	0.0061(4)
F1	4*c*	1	0.0612(6)	3/4	0.8826(6)	0.0061(4)
F2	4*c*	1	0.8653(6)	3/4	0.5240(6)	0.0061(4)

Table S14. Selected interatomic distances (Å) for $Li_{1.68}Na_{0.32}FePO_4F$.

Bond		Bond	
Na1-O1	2.233(8)	Fe1-O1	2.055(4) ×2
Na1-O3	2.111(9)	Fe1-O6	2.158(6) ×2
Na1-O4	2.314(13)	Fe1-F1	2.178(5) ×2
Na1-O5	2.171(11)		
Na1-F1	2.591(12)	Fe2-O2	2.173(4) ×2
Na1-F2	2.530(10)	Fe2-O4	2.056(5) ×2
		Fe2-F2	2.173(4) ×2
Li2-O2	2.58(3)		
Li2-O3	1.80(2)	P1-O1	1.504(5) ×2
Li2-O4	2.147(15)×2	P1-O2	1.497(8)
Li2-F1	1.82(3)	P1-O3	1.482(8)
Li2-F2	2.69(4)		
		P2-O4	1.529(6) ×2
Li3-O1	2.210(13) ×2	P2-O5	1.591(10)
Li3-O5	1.91(3)	P2-O6	1.530(11)
Li3-O6	2.43(3)		
Li3-F1	2.95(3)		
Li3-F2	1.69(3)		

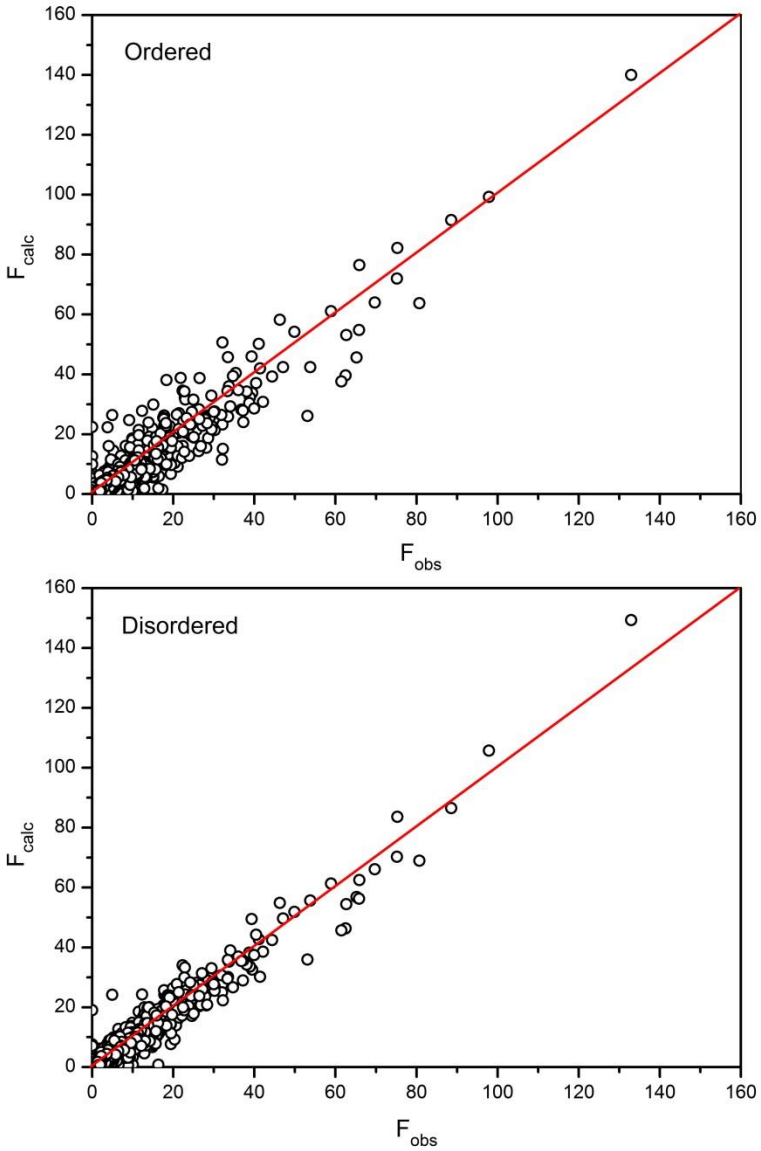

Figure S5. F_{obs}-F_{calc} plots for the ordered (top) and disordered (bottom) Li_2FePO_4F-75 structure models.

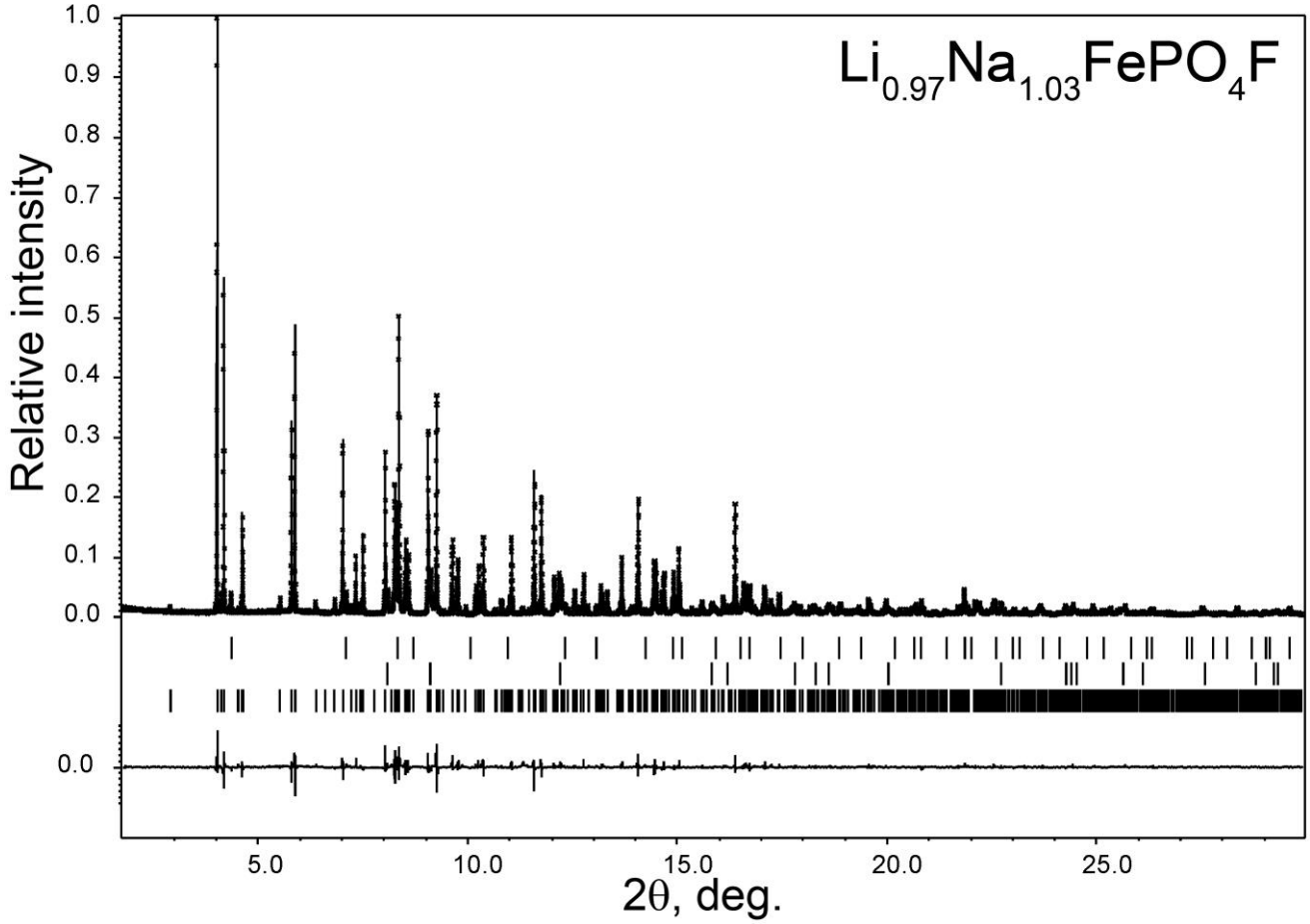

Figure S6. Experimental, calculated and difference SXPD profiles after Rietveld refinement of the $Li_{0.97}Na_{1.03}FePO_4F$ structure. The bars (from top to bottom) mark the reflection positions for Na_2WO_4, WC and $Li_{0.97}Na_{1.03}FePO_4F$.

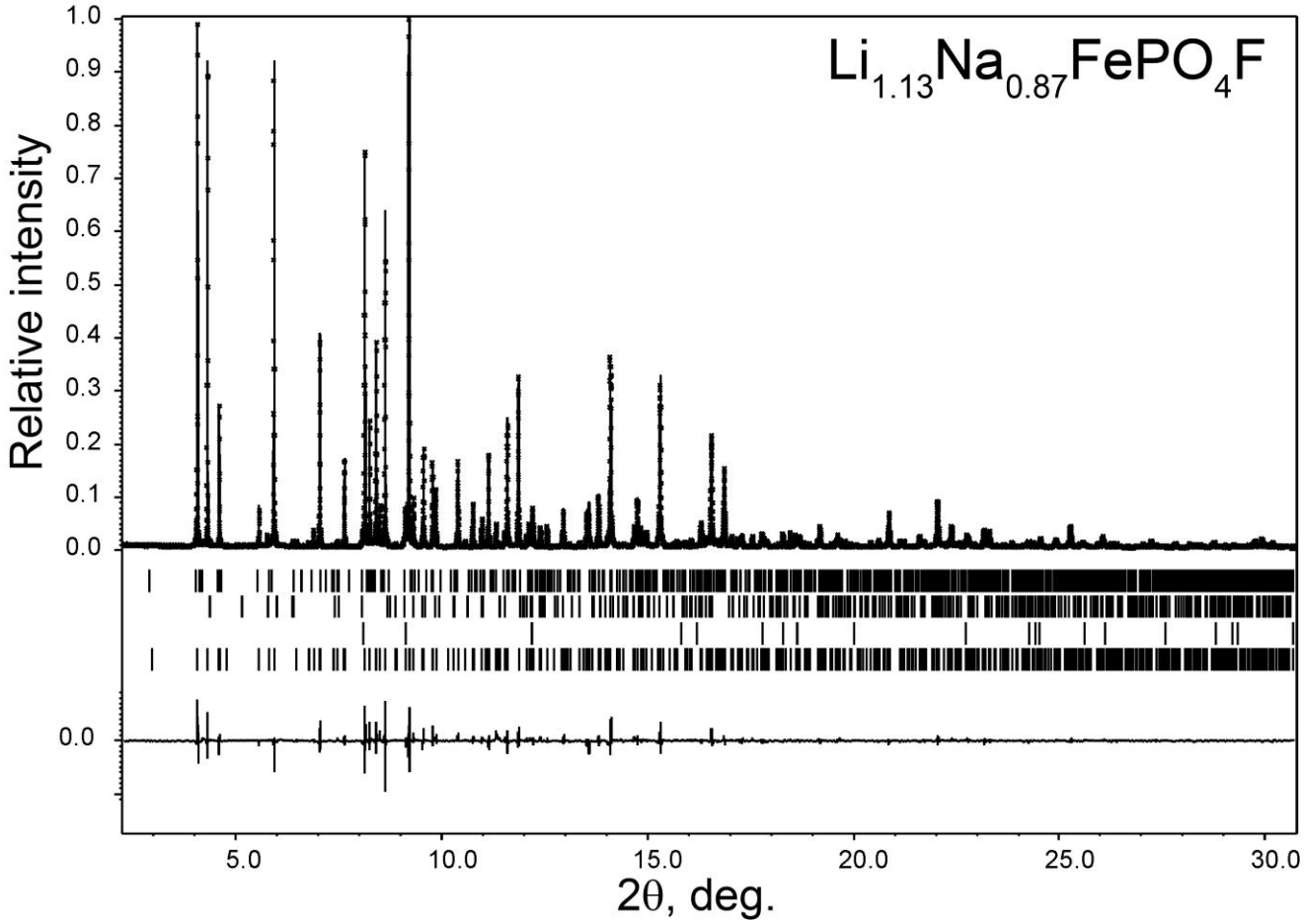

Figure S7. Experimental, calculated and difference SXPD profiles after Rietveld refinement of the $Li_{1.13}Na_{0.87}FePO_4F$ structure. The bars (from top to bottom) mark the reflection positions for $LiNaFePO_4F$, Li_3PO_4, WC and $Li_{1.13}Na_{0.87}FePO_4F$.

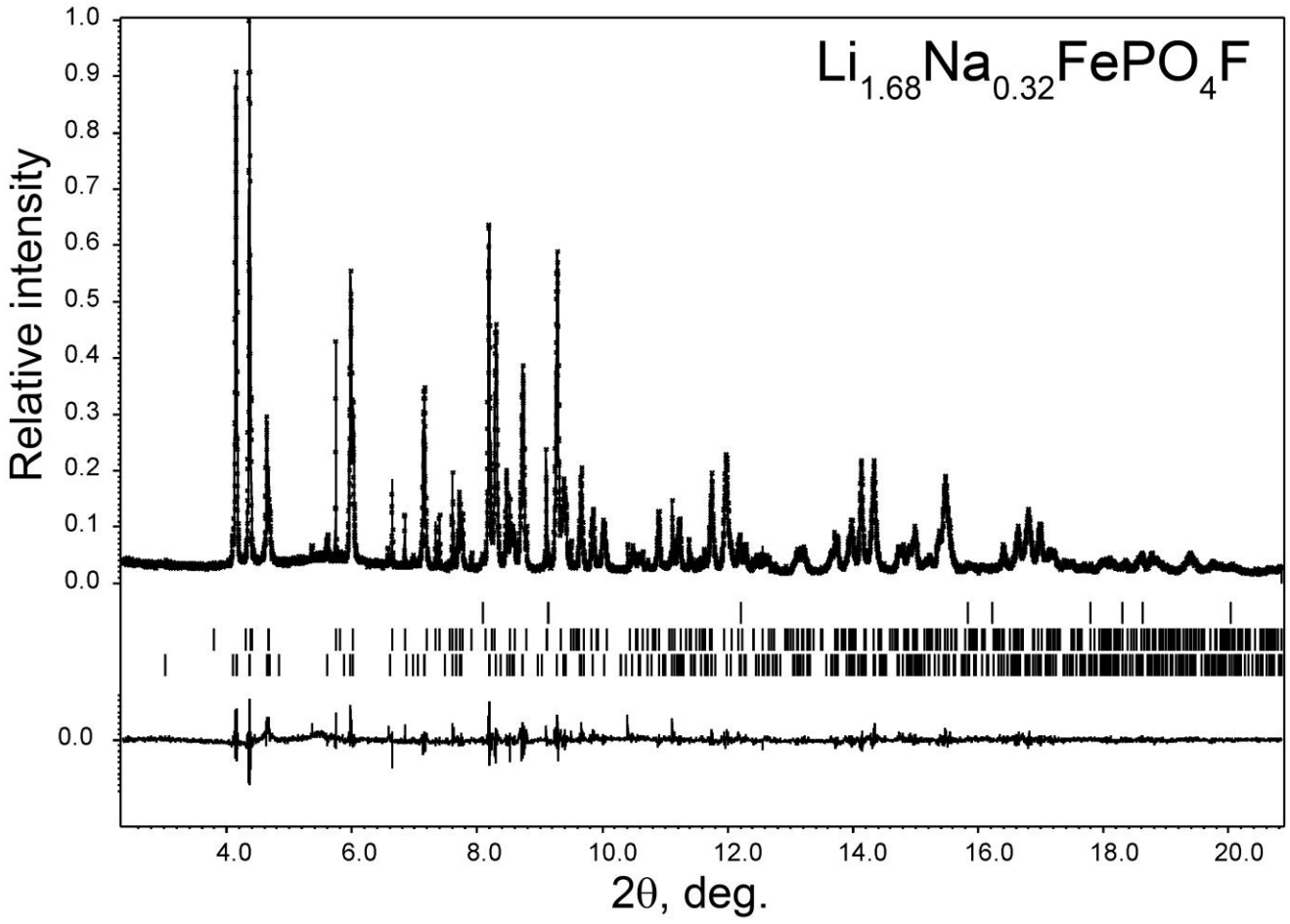

Figure S8. Experimental, calculated and difference SXPD profiles after Rietveld refinement of the $Li_{1.68}Na_{0.32}FePO_4F$ structure. The bars (from top to bottom) mark the reflection positions for WC, $NaBr{\cdot}2H_2O$ and $Li_{1.68}Na_{0.32}FePO_4F$.

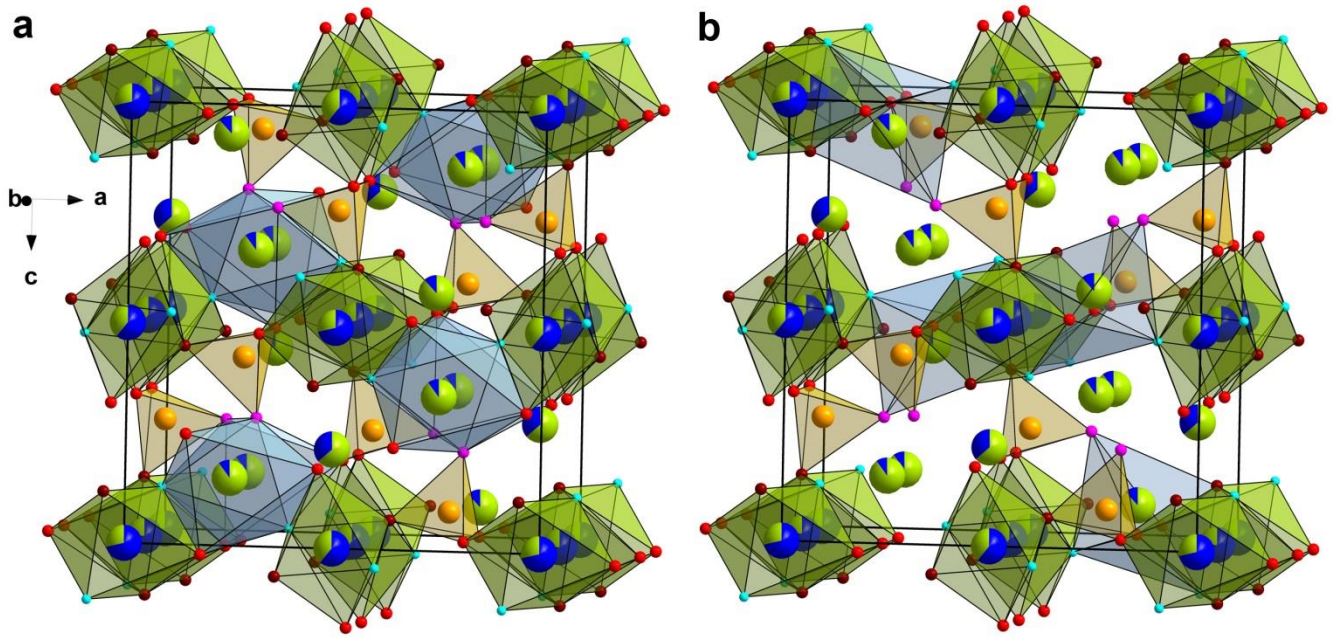

Figure S9. The coordination polyhedra (blue) around the Li1 (a) and Li3 (b) positions in the Li_2FePO_4F-75 crystal structure. See Fig.2a for the legend.

REFERENCES.

(1) Petricek, V.; Dusek, M.; Palatinus, L. Crystallographic Computing System JANA2006: General features. *Z. Kristallogr*. **2014** 229, 345-352.
(2) Palatinus, L. (2011). PETS – program for analysis of electron diffraction data. Prague: Institute of Physics of the AS CR.
(3) Khasanova, N. R.; Drozhzhin, O. A.; Storozhilova, D. A.; Delmas, C.; Antipov, E. V. New form of Li_2FePO_4F as cathode material for Li-ion batteries. *Chem. Mater*. **2012** 24, 4271−4273.]
(4) Kresse, G.;J. Furthmüller, J. Efficiency of ab-initio total energy calculations for metals and semiconductors using a plane-wave basis set. *Comput. Mater. Sci.* **1996** 6, 15-50.
(5) Kresse, G.;J. Furthmüller, J. Efficient iterative schemes for *ab initio* total-energy calculations using a plane-wave basis set. *Phys. Rev. B* **1996** 54, 11169.
(6) Perdew, J.P.; Burke, K.; Ernzerhof, M. Generalized Gradient Approximation Made Simple. *Phys. Rev. Lett.* **1996** 77, 3865.
(7) Hoang, K.; Johannes, M.D. Tailoring Native Defects in $LiFePO_4$: Insights from First-Principles Calculations. *Chem. Mater*. **2011** 23, 3003-3013.
(8) Islam, M. S.; Driscoll, D. J.; Fisher, C. A. J.; Slater, P. R. Atomic-Scale Investigation of Defects, Dopants, and Lithium Transport in the $LiFePO_4$ Olivine-Type Battery Material. *Chem. Mater*. **2005** 17, 5085-5092.